

WFC3/UVIS CTE-EPER Measurement

V. Kozhurina-Platais, B. Hilbert, A. Martel, & P. McCullough

June 21, 2009

Abstract

We present an analysis and the measurements of the Charge Transfer Efficiency (CTE) using the Extended Pixel Edge Response (EPER) technique for the WFC3 UVIS flight detector tested during the ground-based thermal vacuum campaign in April 2008. We present an algorithm for CTE calculation and a power-law functional dependence between CTE and signal level. The analysis shows that CTE is approximately 0.999999 for each amplifier. These CTE pre-flight measurements will serve as a first epoch for WFC3/UVIS CTE internal monitoring.

1. Introduction

It is a well-known fact that there is a significant loss of Charge Transfer Efficiency (CTE) for all HST CCDs in the environment of space: WFPC2 (Whitmore *et al.* 1999, Dolphin 2000), STIS (Gilliland *et al.* 1999; Goudfrooij & Kimble 2003; Goudfrooij *et al.* 2007) and ACS (Riess 2003; Mutchler & Siriani 2005). The CTE losses degrade the CCD detectors with time particularly in space when cosmic rays damage the silicon lattice. The degradation of the CCD detectors due to CTE loss affects the precision of stellar photometry and astrometry on many HST science programs (Riess & Mack 2004; Kozhruina-Platais *et al.* 2007; Kozhurina-Platais *et al.* 2008; Chiaberge *et al.* 2009). Therefore it is important to collect pre-flight measurements of the CTE as a baseline for future measurements of CTE loss in space.

In this paper we report CTE measurements for the new instrument *Wide Field Camera 3* (WFC3), a fourth - generation imaging instrument which was installed in HST during Servicing Mission 4 in May 2009. A popular technique of CTE measurement is the Extended Pixel Edge Response (*EPER*) described by Janesick (2001). *EPER* measures the excess charge in the CCD overscan pixels (extended pixel region), which appears as an exponential tail. The *EPER* technique has been successfully used for the ACS Wide Field Camera and High Resolution Camera to measure and monitor CTE (Mutchler & Sirianni, 2005). The same technique was used by Robberto (2007) to measure CTE for the *WFC3 UVIS-2* detector during the ground-based ambient test campaign in April 2007. Here, we use observations for the flight detector *UVIS-1* taken during the Thermal Vacuum 3 (TV3) test on April 10, 2008.

2. Observations and Reduction

The data were collected during the thermal vacuum calibration test performed at the Goddard Space Flight Center, in April 2008. The CCDs were operated at the nominal flight temperature of T=-83C. The flat field observations were exposed with the internal TUNGSTEN-3 lamp.

In order to achieve a large range of signal levels, the exposures were taken through three filters with integration times tuned for a range of signal levels from 100 e⁻ to 3000 e⁻. Table 1 lists the frame numbers, the consecutive order in observations, the filters and the exposure times used to generate the average signal levels in the flat fields images.

Table 1: The list of frames with WFC3 UVIS filters and exposure time.

Image ID	Trial	WFC3 UVIS Filters	Exp.Time (sec)	Intended Level (e ⁻)	Measured Level (e ⁻)
57190	1	CLEAR	0.5	-	-
57191	2	CLEAR	0.5	-	-
57192	1	F390M	9.2	100	100
57193	2	F390M	9.2	100	101
57194	1	F390M	22.9	250	250
57195	2	F390M	22.9	250	251
57196	1	F390W	6.4	500	500
57197	2	F390W	6.4	500	502
57198	1	F438W	7.6	1000	1001
57199	2	F438W	7.6	1000	1002
57200	1	F438W	22.7	3000	2993
57201	2	F438W	22.7	3000	2993

The Flight Software does not allow for a true bias (with exposure time equal 0) to be taken in EPER mode, therefore the dark exposure could be used as a bias. Thus, the first two images (57190 & 57191) listed in Table 1, are dark exposure with 0.5sec, were used as bias reference images. As can be seen in Table 1, the bias and flat field images were taken in pairs. For analysis purposes, we separated the data into two sets. One set comprised the first image of each pair, while the other contained the second image from each pair. These two data sets were kept separate throughout the analysis. We subsequently refer to these data-sets as *first* and *second* trials.

Before describing data reduction techniques, we outline here the WFC3 CCD detector format and its structure as they relate to EPER measurements. As described in the WFC3 Instrument Handbook for Cycle 17 (Bond *et al.* 2007), each of the UVIS CCD detectors has a size of 4096×2051 pixels. Both CCD chips have 25 extra columns on each side of the detectors, which form the serial physical overscan regions. Each CCD chip also has 30×2 virtual serial overscan areas in the center of each row. Next to the inter-chip gap there are 19 rows of parallel overscan for each CCD chip. Figure 1 shows the format of a raw image obtained with full-chip four-amplifier readout.

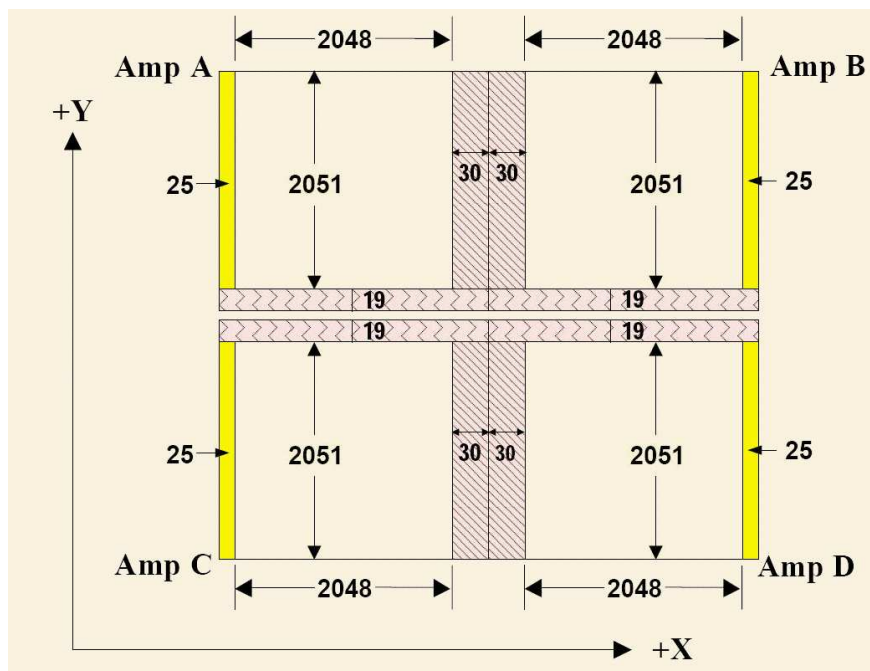


Fig. 1.— Schematic illustration of the standard WFC3 UVIS image from Figure 6.1 of the WFC3 Instrument handbook (Bond *et al.* 2007). The pale yellow color indicates CCD image area (science pixels). The bright yellow color shows serial physical overscan and the pink color indicates serial virtual and parallel virtual overscan.

For EPER measurements, the overscan regions have been modified and contain up to 300 pixels of serial overscan for each CCD chip, and 300 pixels of parallel overscan for each CCD chip. Figure 2 shows the format of an EPER sub-array. As can be seen, the CCD image area associated with each amplifier (indicated by yellow color) is only 1635×1770 pixels. Pixels which are not read out are shown in white.

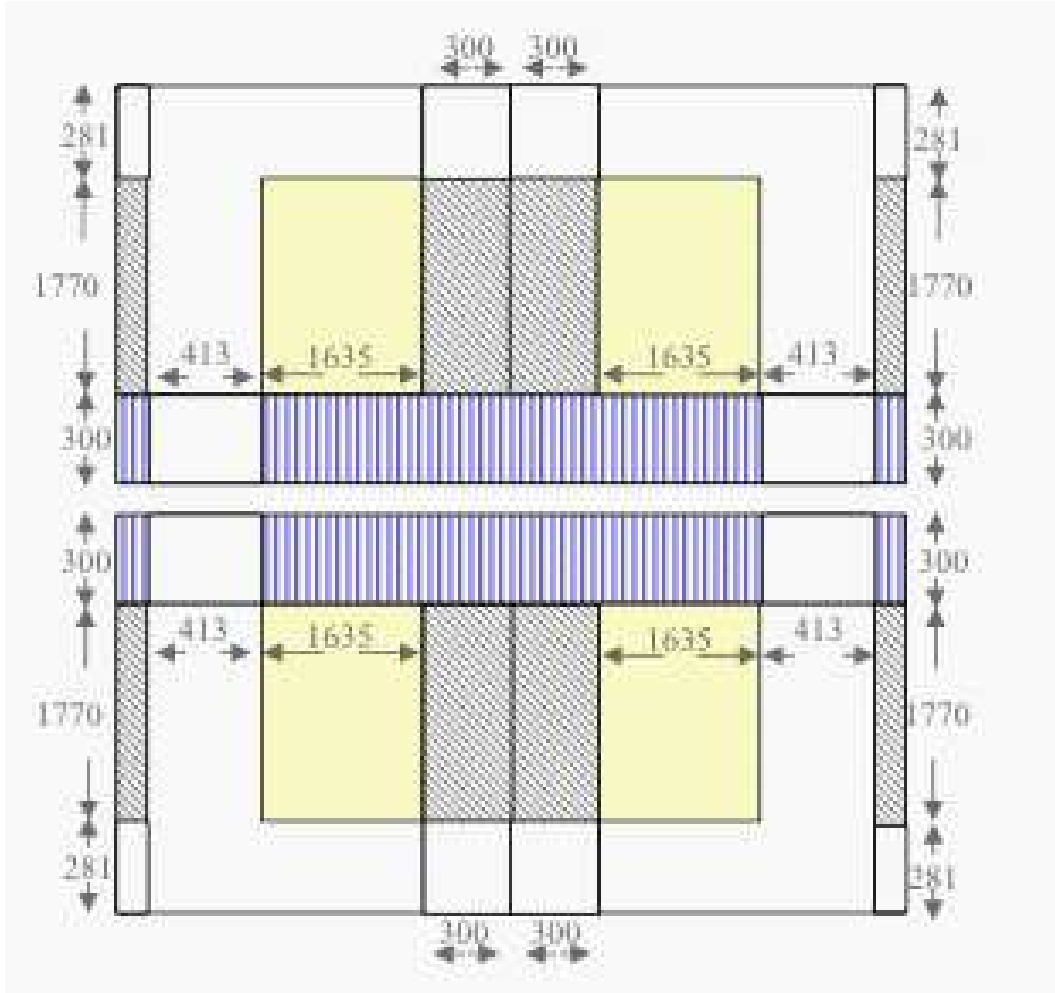


Fig. 2.— Schematic illustration of the EPER WFC3/UVIS sub-array from Robberto (2007, Figure 2). The yellow color indicates the CCD image area while the white color indicates areas that are not read. The blue vertical stripes show the area of the parallel virtual overscan and the grey color denotes areas of serial virtual overscan.

Following the EPER technique described by Janesick (2001), we measure the amount of deferred charge in the extended pixel region. Several lines are averaged to reduce noise and improve the signal-to-noise ratio in the extended pixel region. Then, CTE is calculated from the ratio of the total deferred charge in the extended pixel region S_D (in e^-) over the charge level of the last column of trailing over-scan region S_{LC} (in e^-), multiplied by $N_p = 2051$, which is the number of signal transfers to the CCD register, namely (Janesick, 2001, Eq. 5.21):

$$CTE_{EPER} = 1.0 - \frac{S_D}{S_{LC} \times N_p} \quad (1)$$

Figure 3 shows the CTE measurements and uncertainties for each individual exposure as a function of the signal level in the last column of the trailing region (S_{LC}), where a different color symbol indicates a different order in the consecutive *trials*. Uncertainties were calculated by dividing the standard deviation of S_D by the denominator in Eq.(1). Appendixes A and B contain the measurements of S_{LC} , S_D , CTE and its uncertainties for first and seconds *trials*.

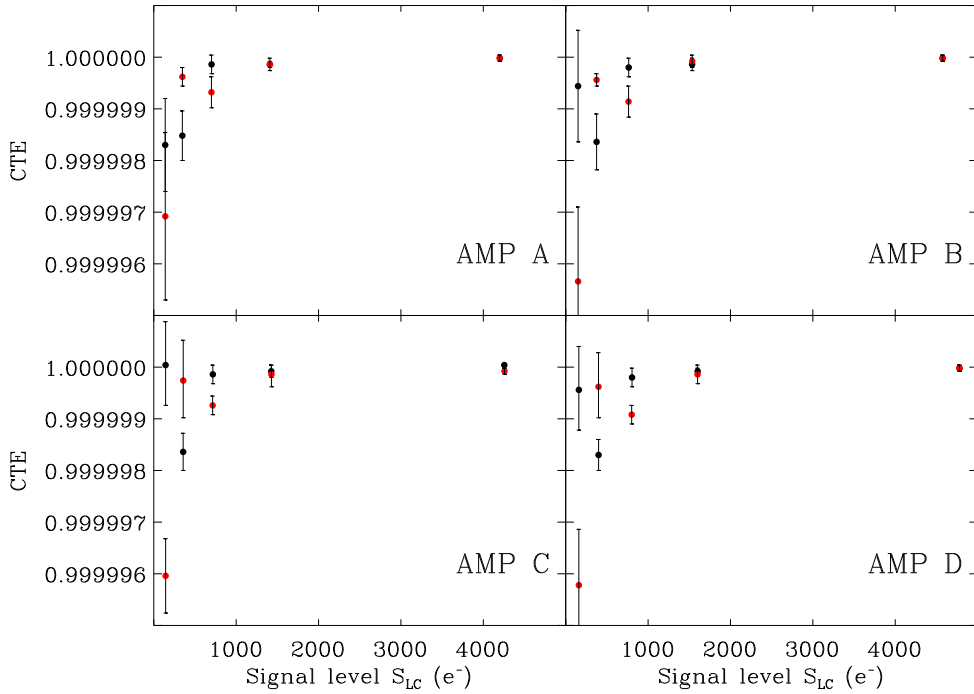


Fig. 3.— UVIS parallel CTE calculated for each individual exposure and for each amplifier. The black symbols show measurements from the first *trial* and the red symbols are from the second *trial*.

As can be seen in Figure 3, there is a noticeable discrepancy in the measurements of CTE between *trials*, particularly for low signal. The discrepancy may be explained by the fact that images with low signal have a large uncertainty in CTE measurements.

3. Power–Law Fit and Linear Fit

As can be seen from Figure 3, CTE improved with increasing signal level and approached the ideal of 1.0 at high signals. The asymptotic distribution of CTE measurements is a clear evidence of a power law relationship between CTE and signal level. The general power law function between two variables follows the polynomial form, namely:

$$f(x) = \epsilon + o(x^\rho) \tag{2}$$

where ϵ is power law constant, and $o(x^\rho)$ is an asymptotically small function of x .

To fit the power law function for CTE as a function of signal level, we redefine function (2) as it was used for ACS/WFC & HRC (Mutchler & Sirianni 2005) and for STIS (Goudfrooij *et al.* 2006) in the following form:

$$CTE = 1 - m \times S^\rho \tag{3}$$

where ρ and m are free parameters and S is the signal level of the last columns in electrons.

Before fitting the power–law function, all exposures taken with the same filter and integration time were averaged. The averaged bias image was subtracted from each averaged flat-field exposure. These averaged exposures were used to fit the power–law function. Equation 3 was solved numerically for each amplifier. The numerical implementation of the power–law fitting was realized by employing a non-linear least-square fit using IDL library by C. Markwardt (2006). The best-fit parameters are listed in Table 2.

Table 2: Parameters of the Power–Law fit.

WFC3 Amplifiers	m	ρ	χ^2
A	3.78e-04±2.9e-04	-1.08±0.11	1.07
B	7.65e-04±7.1e-04	-1.16±0.14	0.92
C	6.04e-04±5.5e-04	-1.11±0.13	0.94
D	8.32e-04±8.0e-04	-1.15±0.16	1.08

Figure 4 shows the CTE calculated from eq.(3) for each averaged exposures as function of signal level, where the solid red line is the best power-law fit.

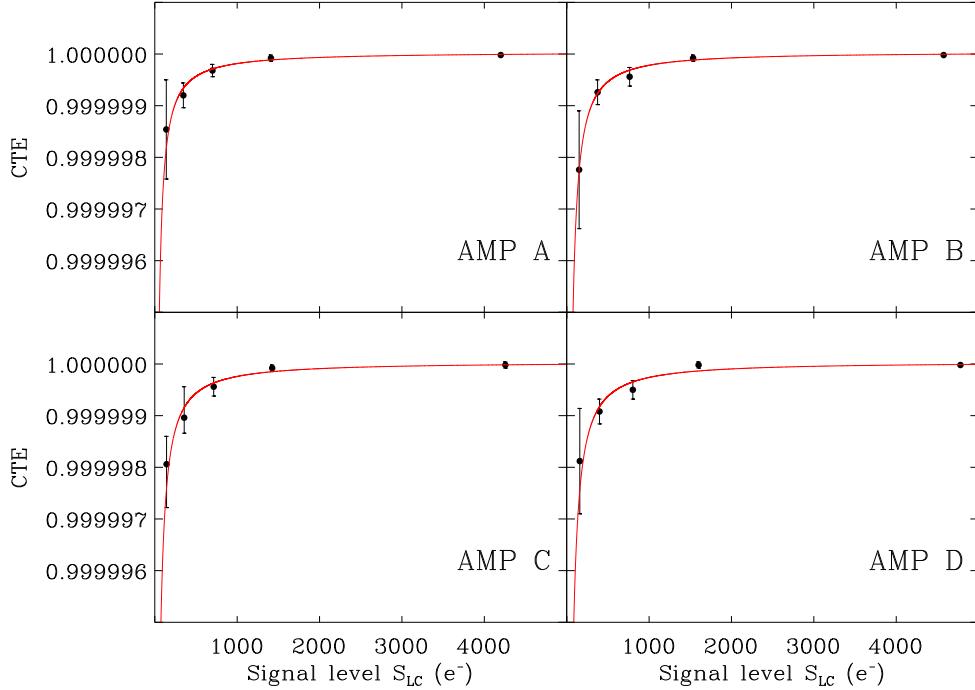


Fig. 4.— UVIS parallel CTE as inferred from EPER data. Over-plotted red line is the best power-law fit.

The parameters listed in Table 2 are identical within the calculated error for all amplifiers. The reduced χ^2 values, close to unity for all amplifiers, mean that the fits are of good quality and leading to the similar fits seen in Figure 4. There is no significant difference in parallel CTE between the four amplifiers.

On the other hand, CTE can be specified in terms of charge transfer inefficiency (CTI), which is the fraction of charge left behind in a single pixel transfer i.e. $CTI = (1 - CTE)$. Then, the equation 3 can be rewritten as linear equation on the \log of parameter m and ρ , namely:

$$\log(CTI) = \log(m) + \rho \times \log(S) \quad (4)$$

Figure 5 shows the CTI calculated from eq.(4) for each amplifier as function of signal level (in e^-), where different symbols show the CTI measurements for all four amplifiers - the asterisk symbols for amplifier A, diamonds for amplifier B, triangles and squares are for amplifiers C & D respectively. The red symbols are the averaged CTI of the four amplifiers and solid red line is the best linear fit of eq.(4).

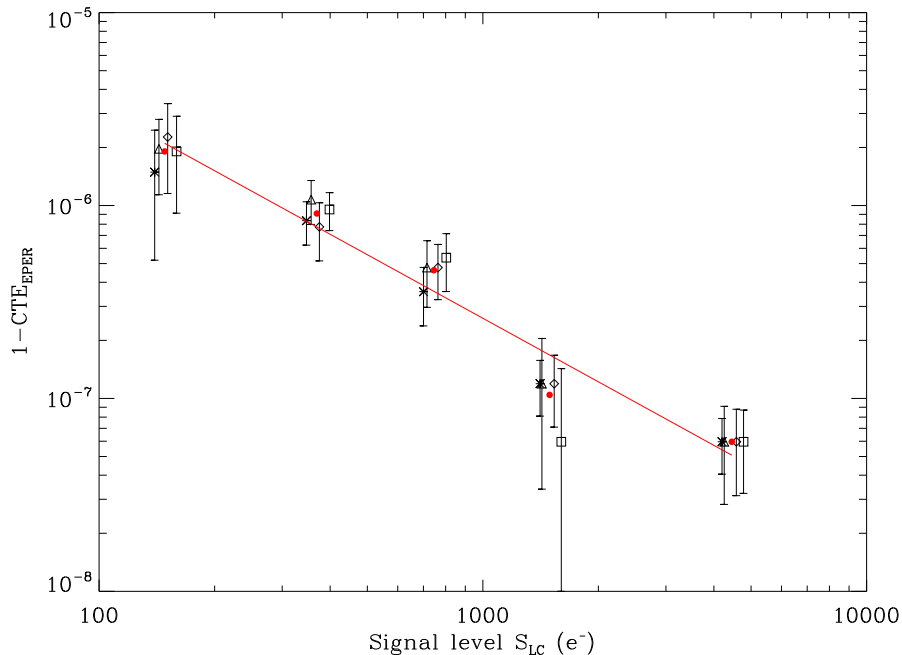


Fig. 5.— UVIS Charge Transfer Inefficiency for all amplifiers, the red symbols show CTI averaged for all 4 amplifiers, and the over-plotted red line is the best linear fit of the averaged CTI.

The best linear least-square fit to the \log of CTE, produce $\log(m) = -3.30 \pm 0.38$ and $\rho = -1.09 \pm 0.13$. Thus, parameters values of m and ρ calculated from non-linear least square fits with a power-law function (Table 2) are consistent with m and ρ calculated from linear least-square fit to the \log of CTE.

The pre-launch parallel CTE measurements for all amplifiers are comparable at *the six nines level*. If assumed that there are no differences between the four amplifiers, then the averaged parameter ρ is equal to -1.12. It is interesting to mention here that for STIS $\rho=-0.82$ (Goudfrooij *et al.* 2006) and for ACS/WFC & HRC $\rho=-0.61$, $\rho=-0.85$ respectively. The different value of ρ for different sensors suggests that this parameter is sensor dependent.

4. Conclusion

This report presents a detailed description of CTE measurements of the WFC3 *UVIS-1* CCDs. The pre-flight measurements of CTE are a prediction of initial inflight WFC3/UVIS performance. The results of CTE measurements will be used as the first epoch of CTE internal monitoring during the inflight calibrations programs. In Cycle 17 calibration

program (GO-11924 – “ WFC3 UVIS External and Internal CTE monitor”), the second component of the program is very similar to pre-flight test during the ground-based thermal vacuum calibration campaign in April 2008. The internal tungsten lamp flat-field will be observed through three filters with a wide range of illumination levels from 100 to 3000 (e^-). The observations will be collected with sufficient frequency through the life of the WFC3/UVIS detector to monitor the CTE degradation with time, and will be useful for the development of future flight CCD detectors.

References

- Bond, H. E., and Kim Quijano, J., et al. 2007, ”Wide Field Camera 3 Instrument Handbook, Version 1.0” (Baltimore: STScI)
- Chiaberge, M., Lim, P.M., Kozhurina-Platais, V., Sirianni, M., Mack, J., 2009, ACS Science Instrument Report 2009-01, (Baltimore: STScI)
- Dolphin, A. E., 2000, PASP, 112, 1397
- Gilliland, R., Goudfrooij, P., Kimble, R., 1999, PASP, 111, 1009
- Goudfrooij, P., & Kimble, R. A., 2003, in “2002 HST Calibration Workshop”, eds. A. Arribas, A. Koekemoer, & B. C. Whitmore (Baltimore: STScI), p.105
- Goudfrooij, P., Bohlin, R. C., & Maíz Apellániz, J., 2006, PASP, 118, 1455
- Janesick, J.R., 2001, “Scientific Charge-Coupled Devices”, SPIE Press, Bellingham VA
- Kozhurina-Platais, V., Goudfroij P., Puzia, T., 2007, ACS Science Instrument Report 2007-04, (Baltimore: STScI)
- Kozhurina-Platais, V., Sirianni, M., Chiaberge, M., 2008, in “Proceedings of IAU Symposium”, Vol. 248, p.272-273
- Markwardt, G. B., in “<http://cow.physics.wisc.edu/craigm/idl/idl.html>”
- Mutchler, M., & Sirianni, M., 2005, , ACS Science Instrument Report 2005-17 (Baltimore: STScI)
- Riess, A., 2003, ACS Science Instrument Report 2003-09 (Baltimore: STScI)
- Riess, A., & Mack, J., 2004, ACS Science Instrument Report 2004-06 (Baltimore: STScI)
- Robberto, M., 2007, WFC3 Science Instrument Report 2007-13,(Baltimore: STScI)
- Whitmore, B. C., Heyer, I., & Casertano, S., 1999, PASP, 111, 1539

Appendix A

The EPER measurements for the *first* trial.

Amplifier	S_{LC}	S_D	CTE
A	$138.9 \pm 1.11e+01$	$0.48 \pm 2.55e-01$	$0.99999829 \pm 8.96e-07$
B	$150.2 \pm 1.23e+01$	$0.18 \pm 3.30e-01$	$0.99999941 \pm 1.07e-06$
C	$143.4 \pm 1.40e+01$	$-0.01 \pm 2.35e-01$	$1.00000002 \pm 7.98e-07$
D	$159.6 \pm 1.54e+01$	$0.15 \pm 2.60e-01$	$0.99999955 \pm 7.94e-07$
A	$346.7 \pm 1.82e+01$	$1.11 \pm 3.36e-01$	$0.99999844 \pm 4.72e-07$
B	$375.0 \pm 2.03e+01$	$1.28 \pm 4.22e-01$	$0.99999833 \pm 5.48e-07$
C	$356.8 \pm 2.46e+01$	$1.22 \pm 2.65e-01$	$0.99999834 \pm 3.63e-07$
D	$399.0 \pm 2.76e+01$	$1.41 \pm 2.50e-01$	$0.99999827 \pm 3.06e-07$
A	$701.4 \pm 2.78e+01$	$0.26 \pm 2.97e-01$	$0.99999982 \pm 2.06e-07$
B	$764.9 \pm 3.35e+01$	$0.35 \pm 2.88e-01$	$0.99999978 \pm 1.83e-07$
C	$717.0 \pm 4.22e+01$	$0.24 \pm 2.56e-01$	$0.99999984 \pm 1.74e-07$
D	$805.1 \pm 4.53e+01$	$0.35 \pm 2.90e-01$	$0.99999979 \pm 1.76e-07$
A	$1409.6 \pm 4.55e+01$	$0.43 \pm 2.56e-01$	$0.99999985 \pm 8.86e-08$
B	$1534.5 \pm 5.72e+01$	$0.46 \pm 2.87e-01$	$0.99999985 \pm 9.13e-08$
C	$1425.9 \pm 7.62e+01$	$0.27 \pm 2.67e-01$	$0.99999991 \pm 9.12e-08$
D	$1601.7 \pm 7.99e+01$	$0.39 \pm 2.79e-01$	$0.99999988 \pm 8.49e-08$
A	$4201.3 \pm 1.10e+02$	$0.62 \pm 3.11e-01$	$0.99999993 \pm 3.61e-08$
B	$4574.7 \pm 1.49e+02$	$0.57 \pm 4.23e-01$	$0.99999994 \pm 4.51e-08$
C	$4254.7 \pm 2.11e+02$	$0.21 \pm 3.52e-01$	$0.99999998 \pm 4.03e-08$
D	$4780.2 \pm 2.14e+02$	$0.42 \pm 4.05e-01$	$0.99999996 \pm 4.13e-08$

Appendix B

The EPER measurements for the *second* trial.

Amplifier	S_{LC}	S_D	CTE
A	$139.4 \pm 1.16e+01$	$0.9 \pm 4.56e-01$	$0.99999693 \pm 1.60e-06$
B	$150.4 \pm 1.24e+01$	$1.4 \pm 4.32e-01$	$0.99999562 \pm 1.40e-06$
C	$143.7 \pm 1.42e+01$	$1.2 \pm 2.17e-01$	$0.99999593 \pm 7.36e-07$
D	$159.6 \pm 1.51e+01$	$1.4 \pm 3.46e-01$	$0.99999578 \pm 1.06e-06$
A	$347.3 \pm 1.83e+01$	$0.3 \pm 1.14e-01$	$0.99999958 \pm 1.61e-07$
B	$374.9 \pm 2.07e+01$	$0.4 \pm 8.36e-02$	$0.99999953 \pm 1.09e-07$
C	$357.4 \pm 2.45e+01$	$0.2 \pm 5.32e-01$	$0.99999971 \pm 7.26e-07$
D	$398.4 \pm 2.64e+01$	$0.4 \pm 4.95e-01$	$0.99999956 \pm 6.06e-07$
A	$699.8 \pm 2.81e+01$	$1.0 \pm 3.92e-01$	$0.99999930 \pm 2.73e-07$
B	$762.8 \pm 3.37e+01$	$1.4 \pm 4.41e-01$	$0.99999913 \pm 2.82e-07$
C	$714.6 \pm 4.15e+01$	$1.1 \pm 2.56e-01$	$0.99999922 \pm 1.74e-07$
D	$801.0 \pm 4.56e+01$	$1.5 \pm 2.91e-01$	$0.99999906 \pm 1.77e-07$
A	$1409.2 \pm 4.47e+01$	$0.5 \pm 3.13e-01$	$0.99999984 \pm 1.08e-07$
B	$1535.5 \pm 5.58e+01$	$0.5 \pm 4.21e-01$	$0.99999986 \pm 1.34e-07$
C	$1428.3 \pm 7.47e+01$	$0.5 \pm 6.31e-01$	$0.99999983 \pm 2.15e-07$
D	$1600.6 \pm 8.01e+01$	$0.6 \pm 6.37e-01$	$0.99999981 \pm 1.94e-07$
A	$4198.7 \pm 1.12e+02$	$0.7 \pm 3.23e-01$	$0.99999992 \pm 3.75e-08$
B	$4576.9 \pm 1.49e+02$	$0.6 \pm 4.25e-01$	$0.99999993 \pm 4.53e-08$
C	$4257.3 \pm 2.12e+02$	$0.7 \pm 6.28e-01$	$0.99999991 \pm 7.19e-08$
D	$4779.2 \pm 2.16e+02$	$0.6 \pm 6.32e-01$	$0.99999994 \pm 6.45e-08$